Gravitational microlensing by the Ellis wormhole

F. Abe

STEL, Nagoya U.

Abe, ApJ, 725, 787-793 (2010)

Presented in SMC2011@Salerno, 22 Jan. 2011

What is wormhole?

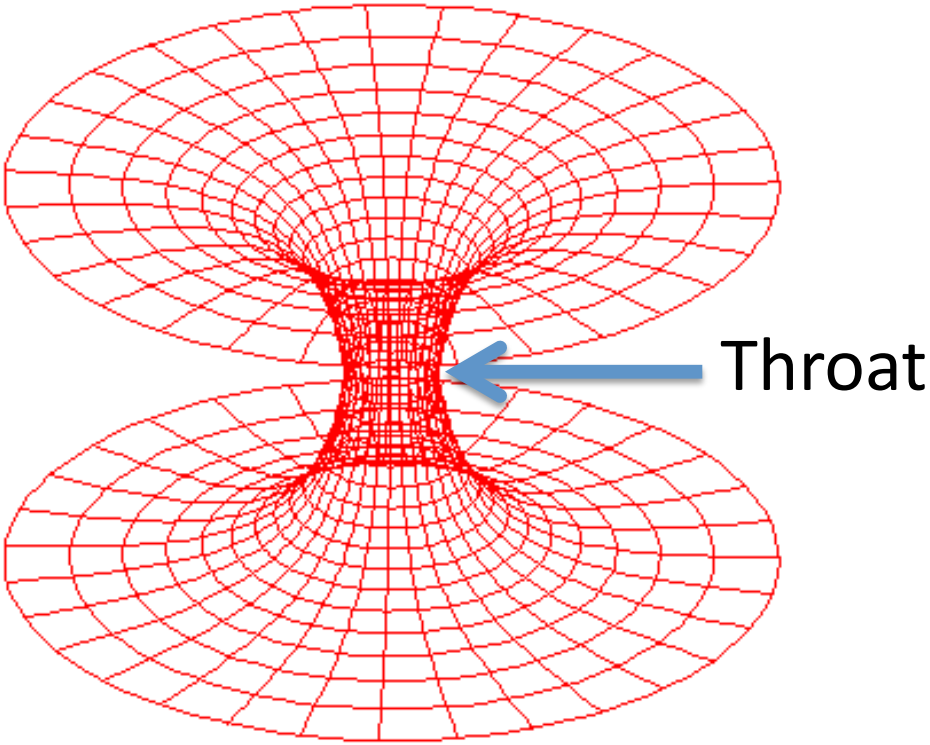

Solutions of Einstein equation that connect distant points in space time. Some of them are traversable（Morris & Thorne 1988）

But existence of them is quite unknown. There has been no reliable method to find them.

Past studies on the methods of finding wormholes

- Gravitational microlensing
  - Cramer et al., 1995 Negative-mass lensing （singular double peaks）
  - Safonova, Torres, Romero 2002, Bogdanov & Cherepashchuk 2008, discussed detectabilities
  - Torres, Romero, Anchordoqui 1998, double-peak gamma ray bursts
- Do wormholes really show negative-mass lensing?

  Not directly derived from space-time structure

Derivations of wormhole lensing as space-time structures

- Rahaman et al., Chinese Journal of Physics, vol. 45, Issue 5, p.518, 2007 C-Field Wormhole
- Nandi et al., Physical Review D, vol. 74, Issue 2, id. 024020, 2006 JNW and Ellis Wormholes
- Dey and Sen, Modern Physics Letters A, Volume 23, Issue 13, pp. 953-962, 2008, derived deflection angle

JNW and Ellis Wormholes

Ellis wormhole (type III)

$$ds^2 = dt^2 - dr^2 - (r^2 + a^2)(d\theta^2 + sin^2(\theta)d\phi^2)$$

a : throat radius

Ellis, H. G. 1973, J. Math. Phys. 14, 104

- Massless scalar field

Morris & Thone 1988, Am. J. Ph. 56, 395

- Traversable

Deflection angle

$$\alpha(r) \to \frac{\pi}{4}\frac{a^2}{r^2} - \frac{5\pi}{32}\frac{a^4}{r^4} + o\left(\frac{a}{r}\right)^6$$

Dey and Sen, 2008

Lensing geometry & Weak-field limit

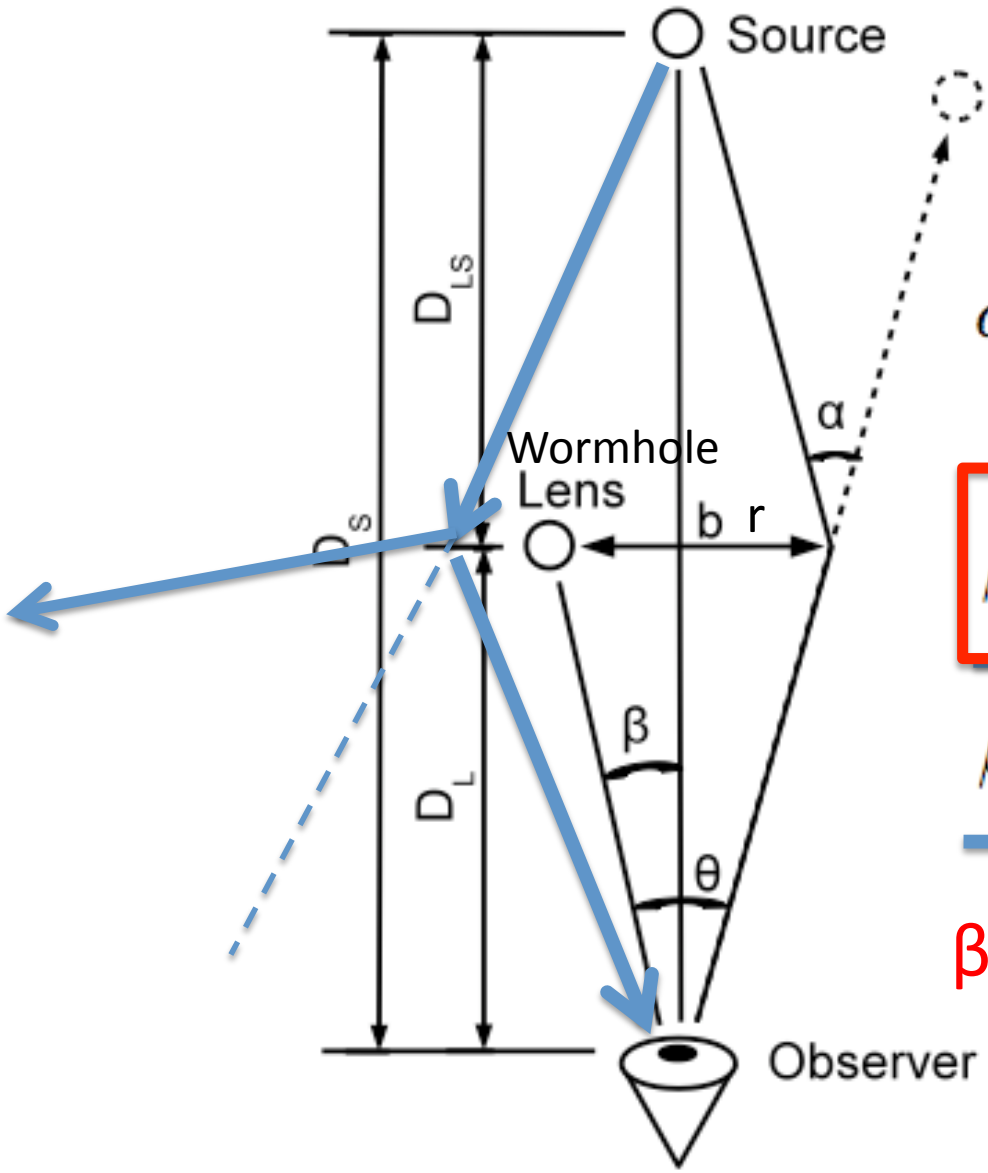

$$\beta = \frac{1}{D_L} b - \frac{D_{LS}}{D_S}\alpha(r)$$

$$\alpha(r) \to \frac{\pi}{4}\frac{a^2}{r^2}$$ Schwarzschild lensin $\frac{4GM}{c^2 r}$

Weak-Field limit

$$\beta = \frac{r}{D_L} - \frac{\pi}{4}\frac{D_{LS}}{D_S}\frac{a^2}{r^2} \qquad (r > 0)$$

$$\beta = \frac{r}{D_L} + \frac{\pi}{4}\frac{D_{LS}}{D_S}\frac{a^2}{r^2} \qquad (r < 0)$$

β = 0

$$R_E = \sqrt[3]{\frac{\pi}{4}\frac{D_L D_{LS}}{D_S}a^2}$$

Einstein radius

Image positions

Cubic equations

$$\hat{\theta}^3 - \hat{\beta}\hat{\theta}^2 - 1 = 0 \qquad (\hat{\theta} > 0)$$

$$\hat{\theta}^3 - \hat{\beta}\hat{\theta}^2 + 1 = 0 \qquad (\hat{\theta} < 0)$$

$$\theta_E = R_E / D_L$$

$$\hat{\theta} = \theta / \theta_E$$

$$\hat{\beta} = \beta / \theta_E$$

The real solutions correspond image positions.

One image is $\hat{\theta} > 0$ and outside the Einstein ring.

The other image is $\hat{\theta} < 0$ and inside the Einstein ring.

Image positions

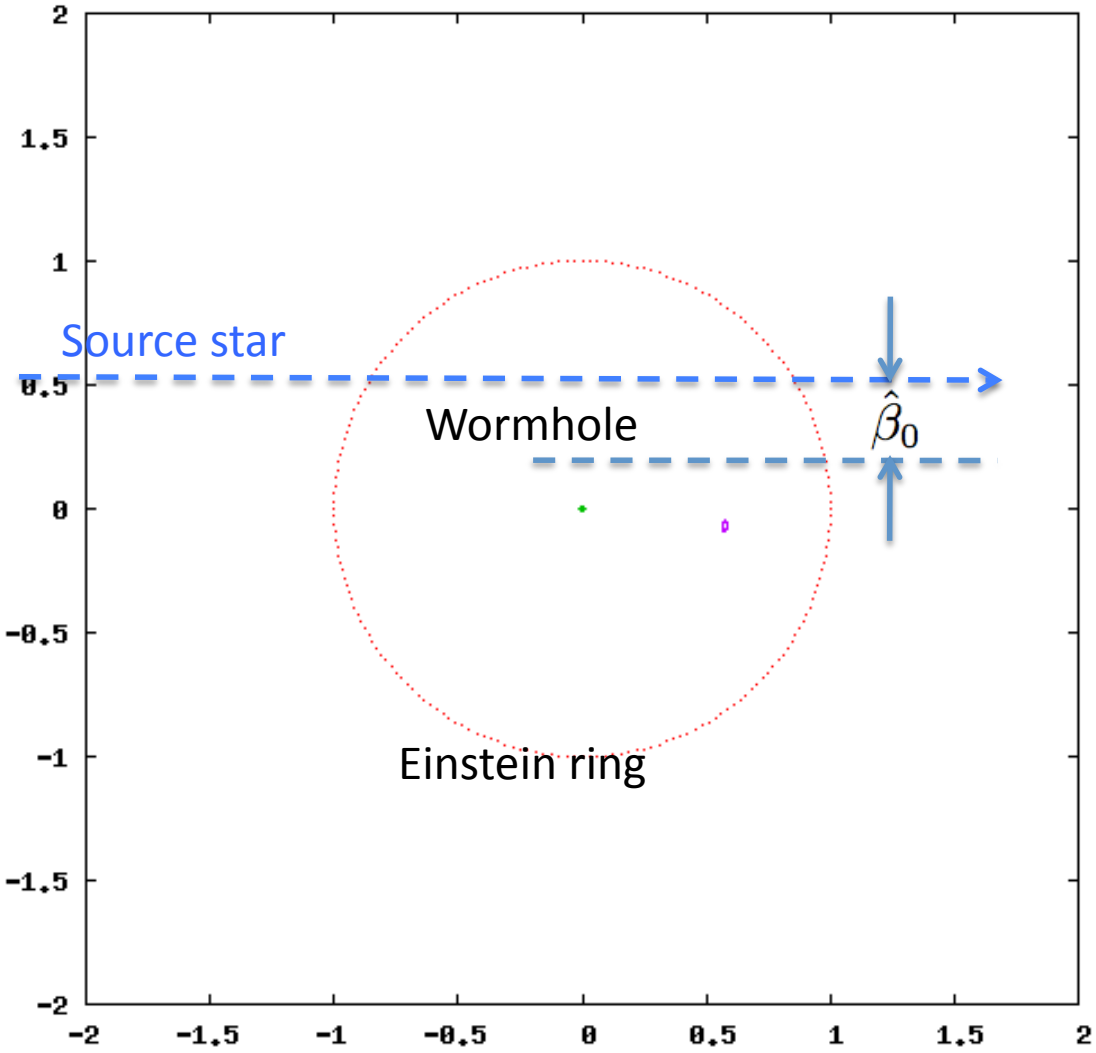

Very similar to the Schwarzschild lensing. But slightly different in the positions and shapes.

Table 1: Einstein radii for bulge and LMC lensings

	Bulge[a]		LMC[b]	
$a(km)$	$R_E(km)$	$\theta_E(mas)$	$R_E(km)$	$\theta_E(mas)$
1	3.64×10^5	0.001	6.71×10^5	< 0.001
10	1.69×10^6	0.003	3.12×10^6	0.001
10^2	7.85×10^6	0.013	1.45×10^7	0.004
10^3	3.64×10^7	0.061	6.71×10^7	0.018
10^4	1.69×10^8	0.283	3.12×10^8	0.083
10^5	7.85×10^8	1.31	1.45×10^9	0.387
10^6	3.64×10^9	6.10	6.71×10^9	1.80
10^7	1.69×10^{10}	28.3	3.12×10^{10}	8.35
10^8	7.85×10^{10}	131	1.45×10^{11}	38.7
10^9	3.64×10^{11}	610	6.71×10^{11}	180
10^{10}	1.69×10^{12}	2 832	3.12×10^{12}	835
10^{11}	7.85×10^{12}	13 143	1.45×10^{13}	3 874

Finite source effect

Typical star radius
7×10^5 km

Direct imaging

Derivation of light curves

$$A = A_1 + A_2 = \left|\frac{\hat{\theta}_1}{\hat{\beta}}\frac{d\hat{\theta}_1}{d\hat{\beta}}\right| + \left|\frac{\hat{\theta}_2}{\hat{\beta}}\frac{d\hat{\theta}_2}{d\hat{\beta}}\right|$$

Conservation of surface brightness

Magnification by image 1 ($\hat{\theta}$>0)

Magnification by image 2 ($\hat{\theta}$<0)

$$= \left|\frac{\hat{\theta}_1}{\hat{\beta}\left(1+\frac{2}{\hat{\theta}_1^3}\right)}\right| + \left|\frac{\hat{\theta}_2}{\hat{\beta}\left(1-\frac{2}{\hat{\theta}_2^3}\right)}\right|$$

$$\hat{\beta}(t) = \sqrt{\hat{\beta}_0^2 + (t-t_0)^2/{t_E}^2}$$

$\hat{\beta}_0$: impact parameter

$$t_E = R_E/v_T$$

Same method as Schwarzschild lensing

Paczynski, ApJ 304, 1, 1986

Light curves

$\hat{\beta}_0$: impact parameter

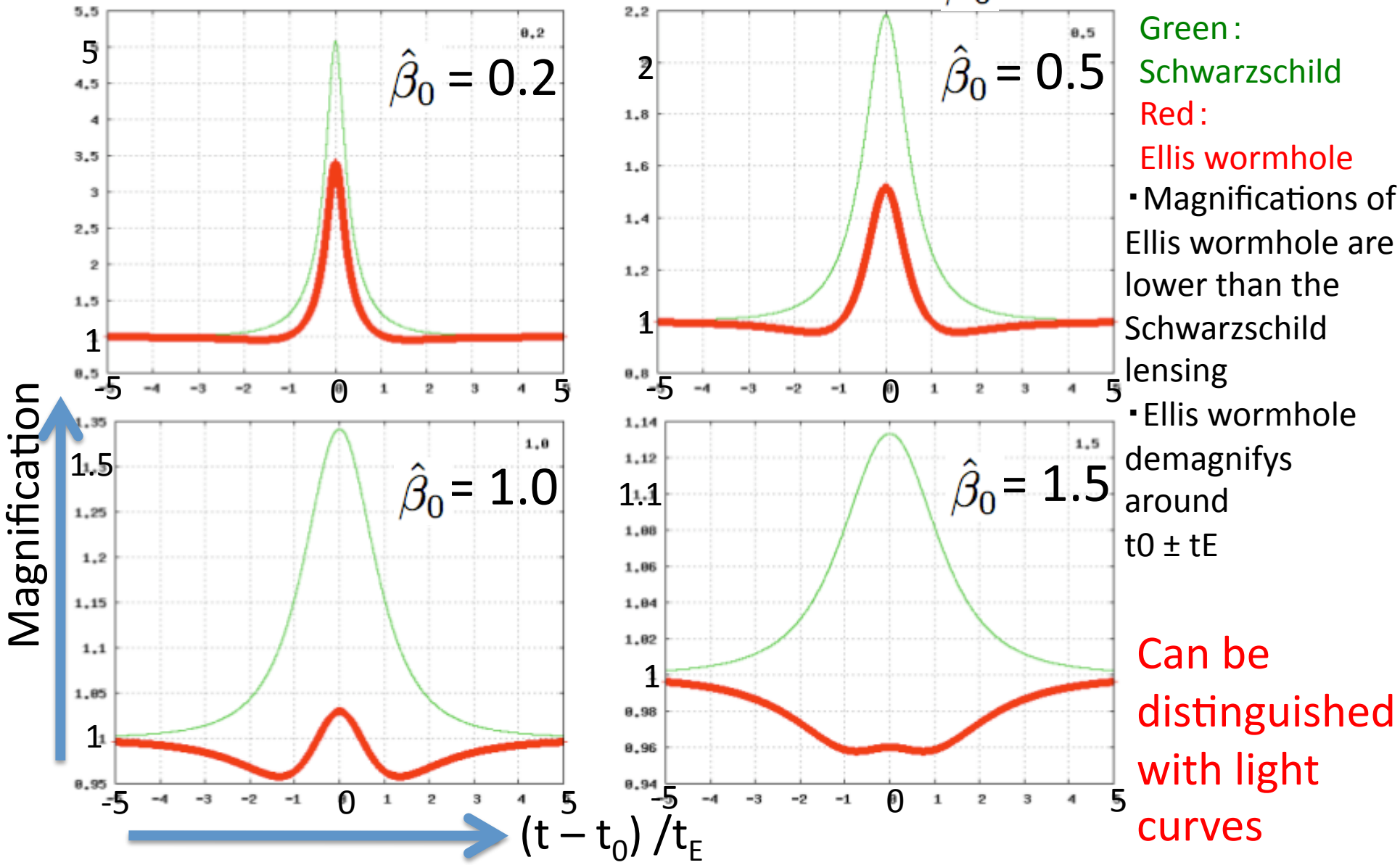

Green : Schwarzschild

Red : Ellis wormhole

- Magnifications of Ellis wormhole are lower than the Schwarzschild lensing
- Ellis wormhole demagnifys around t0 ± tE

Can be distinguished with light curves

Table 2: Einstein radius crossing times for bulge and LMC lensings

	Bulge[a]		LMC[b]	
$a(km)$	$t_E(day)$		$t_E(day)$	
	Bound[c]	Unbound[d]	Bound[c]	Unbound[d]
1	0.019	0.001	0.035	0.002
10	0.089	0.004	0.164	0.007
10^2	0.413	0.018	0.761	0.033
10^3	1.92	0.084	3.53	0.155
10^4	8.90	0.392	16.4	0.721
10^5	41.3	1.82	76.1	3.35
10^6	192	8.44	353	15.5
10^7	890	39.2	1 639	72.1
10^8	4 130	182	7 608	335
10^9	$> 10^4$	843	$> 10^4$	1 553
10^{10}	$> 10^4$	3915	$> 10^4$	7 212

Limited by cadence

Limited by period

Assumptions

Bound model:

v_T = 220 km/s

Unbound model:

v_T = 5000 km/s

Optical depth

$$\tau = \pi \int^{D_S} n(D_L) R_E^2 dD_L$$

$N(D_L)$: number density

$$\begin{aligned}
\tau &= \pi n \int_0^{D_S} \frac{\pi}{4} \left[\frac{D_L(D_S - D_L)}{D_S} a^2 \right]^{2/3} dD_L, \\
&= \sqrt[3]{\frac{\pi^5}{2^4}} n a^{4/3} D_S^{5/3} \int_0^1 [x(1-x)]^{2/3} dx, \\
&\approx 0.785 n a^{4/3} D_S^{5/3}.
\end{aligned}$$

No prediction on n

Assumptions:

Bound : $n = \rho_{Ls} / \langle M_{star} \rangle = 0.147 pc^{-3}$

Bound to the Galaxy (local stellar density)

Unbound : $n = \rho_c \Omega_b \rho_{Ls} / (\rho_{Lb} \langle M_{star} \rangle) = 4.97 \times 10^{-9} pc^{-3}$

Unbound. Uniformly distributed in the universe.

Event rate

$$\begin{aligned}\Gamma &= 2\int_0^{D_S} n(D_L) R_E v_T dD_L \\ &= \sqrt[3]{2\pi} n v_T D_S^{4/3} a^{2/3} \int_0^1 \sqrt[3]{x(1-x)} dx \\ &\approx 0.978 n v_T a^{2/3} D_S^{4/3}\end{aligned}$$

Assumptions:

Bound : $n = \rho_{Ls}/\langle M_{star}\rangle = 0.147 pc^{-3}$

Unbound : $n = \rho_c \Omega_b \rho_{Ls}/(\rho_{Lb}\langle M_{star}\rangle) = 4.97 \times 10^{-9} pc^{-3}$

Table 4: Optical depths and event rates for LMC lensing

	Bound[a]		Unbound[b]	
$a(km)$	τ	$\Gamma(1/year)$	τ	$\Gamma(1/year)$
10	1.75×10^{-10}	2.82×10^{-7}	5.90×10^{-18}	2.17×10^{-13}
10^2	3.76×10^{-9}	1.31×10^{-6}	1.27×10^{-16}	1.01×10^{-12}
10^3	8.11×10^{-8}	6.07×10^{-6}	2.74×10^{-15}	4.67×10^{-12}
10^4	1.75×10^{-6}	2.82×10^{-5}	5.90×10^{-14}	2.17×10^{-11}
10^5	3.76×10^{-5}	1.31×10^{-4}	1.27×10^{-12}	1.01×10^{-10}
10^6	8.11×10^{-4}	6.07×10^{-4}	2.74×10^{-11}	4.67×10^{-10}
10^7	1.75×10^{-2}	2.82×10^{-3}	5.90×10^{-10}	2.17×10^{-9}
10^8	3.76×10^{-1}	1.31×10^{-2}	1.27×10^{-8}	1.01×10^{-8}
10^9	8.11	6.07×10^{-2}	2.74×10^{-7}	4.67×10^{-8}
10^{10}	175	2.82×10^{-1}	5.90×10^{-6}	2.17×10^{-7}

Detectable

Undetectable

Number of stars monitored: 10^6

If no candidates found, we can set limits on the abundance

Summay

- Light curves of gravitational microlensing by the Ellis wormhole are calculated.
- The light curves have characteristic gutters immediately outside the Einstein ring crossing times.
- Ellis wormhole lensing demagnifys at the gutters.
- Optical depths and event rates are calculated in bound and unbound hypotheses.
- The results show bound wormholes can be detected from past LMC data if the throat radius is between 100 to 10^7 km.